Implementation and evaluation of control strategies based on an open controller for a 10 MW floating wind turbine

Ruiqi Hu[a,b], Conghuan Le[a,b*], Zhen Gao[a,b], Hongyan Ding[a], Puyang Zhang[a]

[a]*State Key Laboratory of Hydraulic Engineering Simulation and Safety, Tianjin University, Tianjin 300072, China*

[b]*Department of Marine Technology, Norwegian University of Science and Technology (NTNU), Trondheim 7491, Norway*

[*]*Corresponding author: leconghuan@163.com*

Abstract. The reliability assessment concerning the drivetrain system is important for integrated dynamic analysis of large-scale floating wind turbines (FWTs). An open, modular, and adaptable baseline wind turbine controller is implemented and evaluated in this paper to work with the DTU 10 MW reference wind turbines supported by a proposed Tension Leg Platform (TLP). Higher natural frequency of the controller can account for the coupling effects between the blade pitch control and the platform motions that contributing to poor performances of the FWT and negative damped pitch motions. Through simulations by FAST code, the baseline controller is evaluated by comparing the conventional pitch-to-feather strategy and the active pitch-to-stall strategy. The controller is detuned with different control frequencies and the active stall control strategy is tailored for the proposed TLPFWT. The results suggests that system instabilities induced by higher control frequency decreases fast as the growth of wind speed and the stall controller can lead to around twice platform motions and structure force as large as baseline controller in a wide range of frequency, whereas the rotor performance is fine. The DRC working with FAST proves applicable and different control algorithms and the integrated dynamic effects with other floating foundations can be achieved.

Keywords: Offshore wind turbine; Blade pitch control; Negative damping; Floating foundation; Active stall control

1. Introduction

Offshore wind energy took its first steps in the 1990s and has been growing in scale ever since. From being 1% of global wind installations by capacity in 2009, offshore wind has grown to over 10% in 2019 [1]. Currently most offshore wind turbines are installed in shallow water with bottom fixed foundations. The floating support platforms are still at an early stage of development. While wind energy on land is cost competitive already, offshore wind power is also forecasted to become competitive in relatively few years [2]. Thus, increased reliability and decreased costs are essential for floating wind turbines especially in deep water. The floating concepts proposed for offshore wind turbines are mainly four categories including the Spar-buoy platform (Spar), Tension-leg platform (TLP), Barge platform (Barge) and Semi-submersible platform (Semi) [3,4,5]. These concepts vary depending on their capability of standing stable in the water: stabilized by ballast (Spar), stabilized by ties (TLP), stabilized by buoyancy (Barge and Semi), as shown in Fig. 1.

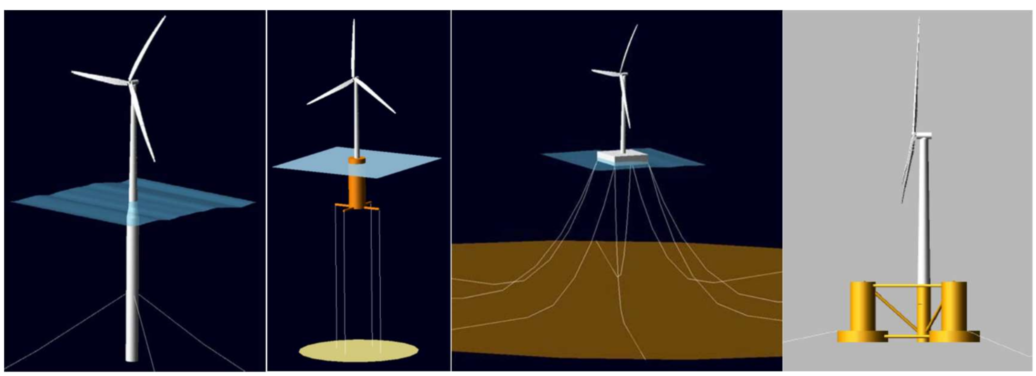

Fig. 1. Illustrations of Floating wind turbines on OC3-Hywind spar buoy, MIT/NREL TLP, ITI Energy barge and OC4-DeepCwind.

Offshore wind turbines consist of a rotor, a drivetrain, an electric generator, and a supporting structure to support the tower. The size of wind turbine has been enlarged to megawatts. The detailed information about the blades, tower and support structures are available for realistic research studies such as the NREL 5MW RWT [6] and DTU 10 MW RWT [7]. Upscaling of wind turbines to harness more wind energy and generate higher electrical power is necessary but challenging because the mass of the turbine increases with the cube of the rotor radius with linear upscaling [7]. In addition, due to higher wind speed and the increased size of the wind turbine, the structural loads or actions can influence the wind. The wind turbine controller can regulate the generator power in variable wind speed by reducing the rotor speed or by pitching the blades and with the variable speed wind turbines, the torque fluctuations on the drive train can be effectively decreased [1,8]. Therefore, the control strategy should be paid with more attention to regulate the power generation and structure dynamic responses. Inspired by the already widely investigated NREL 5MW RWT, the light rotor DTU 10 MW RWT is chosen for this paper to evaluate the controller coupled effects.

The main goal of the controller is to modify the operating states of the turbine to maintain safe operation, maximize power capture, mitigate damaging fatigue loads, and detect fault conditions [9,10]. The control strategies can be categorized as the active control and the passive control. Regarding the active control, pitch variable-speed wind turbine controller has become the dominating type in recent years [10,11]. Typically for the variable-speed pitch control, two controllers are applied including the generator torque control for low wind speed and blade pitch control for overrated wind speed. As for the blade pitch control, variable power collective pitch control and individual pitch control for load mitigation of floating offshore wind turbines are proposed, and applied to the NREL 5 MW RWT models which modifies the rated generator speed to a variable depending on the platform pitch velocity [12-17]. The possibility of using individual pitch control was suggested being capable of reducing the dominant load peak on the blades better than collective pitch control does, but it has not yet fully commercial accepted [14-17].

The main problem associated with the control of floating wind turbines is related to instability of the system in full load [18-20]. The blade pitch angle of active blade pitch controller increases as the wind speed increases in the overrated region to reduce rotor speed and rotor thrust force. The drop in steady-state rotor thrust with overrated wind speed would lead to negative damping and contribute to the large system-pitch motions [6,18]. However, these issues involved in large scale floating wind turbines are not clear yet for many reasons. The most important one is that many research groups generally use self-developed control implementations and tunings and some has provided with an open source controller, for instance the NREL for its NREL 5 MW RWT and the DTU for its DTU 10-MW RWT [6,21,22]. However, these controllers either unavailable or limited in functions which makes the extension and estimation more difficult and inconvenient. Therefore, it is important to find an available and modifiable controller to conduct various simulations without computer compiling background.

The main contribution of this paper is implementing different control strategies with the DRC (Delft Research Controller) baseline controller to work with the DTU 10 MW RWT and estimating its dynamic performance by considering a proposed TLP floating foundation. The DRC baseline controller is developed by the research group from Delft University of Technology to provide an open, modular, and fully adaptable baseline wind turbine controller which can be applied to all turbine models if the Bladed-style DISCON controller interface is used [21,23]. The control parameters used in DRC are verified with the descriptions given by basic DTU wind energy controller [22]. Further modifications of the DRC baseline controller are inspired by the negative damping issues discussed in controlling of NREL 5 MW RWT and based on the classical proportional-integral (PI) control theory [18,24,25].

The organization of this paper is as follows. The introduction of the offshore wind turbines and the control issues for large scaled wind turbines is described at first, which leads to the application of the DRC baseline controller for the following simulations. In Section 2, aerodynamics and dynamic motions of DTU 10 MW RWT and more detailed discussion on the negative damping is given. The geometric parameters of RWT and the proposed TLP platform is also provided. The DRC baseline controller and PI gain schedule are described in Section 3 with the active stall control method which are tested in the following Section. In Section 4, simulation results of the DTU 10 MW RWT with TLP platform controlled by the DRC are shown and discussed. Conclusions are drawn at last. The plots of DTU 10 MW RWT and the proposed TLP platform geometry are shown in Fig.2.

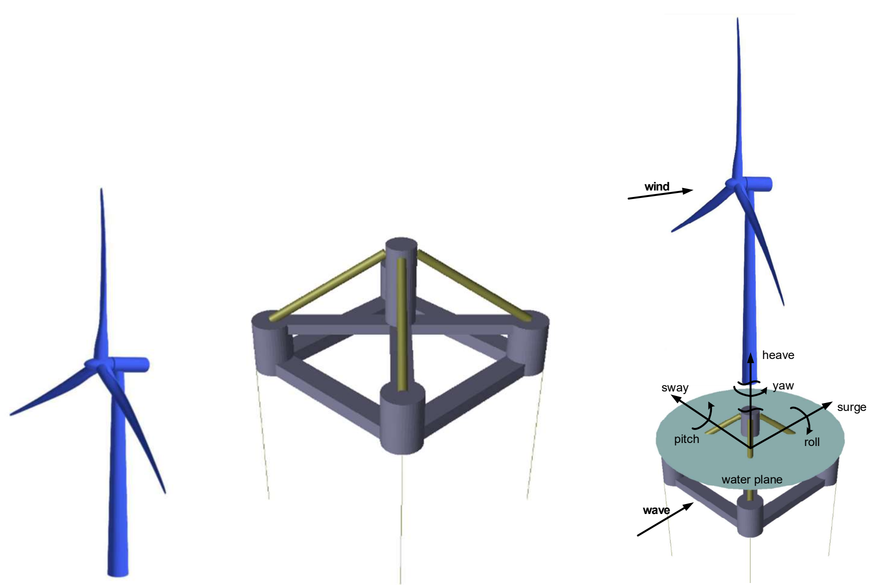

Fig. 2. Plots of the DTU 10MW RWT geometry [17], the TLP platform geometry and the

floating wind turbine system.

Remark: although this paper focuses on the control of a TLP floating type, the controller and implemented methods are applicable to offshore wind turbines with other floating foundations.

2 Numerical Modeling of DTU 10 MW Floating Wind Turbine

The FAST (Fatigue, Aerodynamics, Structures and Turbulence) code developed by NREL (National Renewable Energy Laboratory) is applied in this paper to cooperate with the DRC baseline controller and conduct dynamic analyses for 10 MW RWT with TLP platform. The control design is mostly related to the wind turbine dominant dynamics. The aerodynamics denotes the power generation by rotor. The nonlinear aeroelastic motion accounts for the time domain dynamic responses of wind turbine system. The geometric parameters about the wind turbine and the floating foundation are provided here.

2.1 DTU 10 MW RWT and TLP platform

The DTU 10 MW RWT has been described in details in DTU report [7]. The key parameters of this reference wind turbine are listed in Table 1. The TLP floating foundation is originally proposed for NREL 5 MW RWT which features in large water plane area facilitating the towing operation and in tension legs to limit the dynamic motions in operation [30-32]. The platform is dragged downward below the water to reduce the wave effects. The original geometry parameters of the TLP foundation are scaled considering stability requirements for being able to support the large size DTU 10 MW RWT. The revised geometric parameters and the system engine frequencies are listed in Table 2. The information on the mooring system is presented in Table 3.

Table 1. Key parameters of the DTU 10 MW RWT [7].

Parameter	DTU 10 MW RWT
Rated power	10 MW
Cut in, Rated, Cut out wind speed	4, 11.4, 25 m/s
Number of blades	3
Rotor Diameter	178.3 m
Hub Diameter, Height, Overhang	5.6 m, 119.0 m, 7.1 m
Minimum, Maximum Rotor speed	6.0 rpm, 9.6 rpm
Maximum Generator Speed	480.0 rpm
Gearbox Ratio	50
Maximum Tip Speed	90.0 m/s

Shaft Tilt Angle	5.0 deg
Rotor Precone Angle	-2.5 deg
Rotor Prebend	3.332 m
Rotor, Nacelle, Tower Mass	227962, 446036, 628442 kg
Blade 1st flap mode, edge mode	0.61 Hz, 0.93 Hz
1st Tower bending mode	0.25 Hz
1P, 3P ranges	0.1 Hz-0.16 Hz, 0.3 Hz-0.48 Hz

Table 2. Key parameters of the TLP platform.

Parameter	Tension Leg Platform
Main Colum Diameter	11 m
Potton Height	4 m
Centre Colum Diameter	8.3 m
Displaced Volume	12516 m^3
Platform Mass (with ballast)	4811.62 t
Platform Inertia	2.31E9, 2.31E9, 4.02E9 kg m^2
Draft / Free board	26 / 11.5 m
Pretension	7111.87 t
Surge / Heave Natural Frequency	0.042 / 0.476 Hz
Pitch / Yaw Natural Frequency	0.243 / 0.062 Hz

Table 3. Properties of the TLP mooring system.

Properties	Value
Number of mooring lines	8
Fairlead distance from center	40.855 m
Unstretched mooring-line length	74.0 m
Line diameter	0.143 m
Line mass per unit length	89.2 kg/m
Line extensional stiffness	1.83E9 N
Pretension	6.98E+07 N

2.2 Aerodynamics

Aerodynamics of a wind turbine model comprise the main aerodynamic characteristics of the blades and the control system strategies and parameters. The aerodynamic behavior of wind turbine blades is accounted for by the blade element momentum (BEM) theory which assumes that the blade can be analyzed by a number of independent elements. It combines the momentum theory and the blade-element theory to determine the induced velocity at each element by the momentum balance on a rotating annular stream tube passing through the blade and examine the forces generated at elements along the blade by the airfoil lift and drag coefficients[26].

In the variable-speed control system, there are mainly three regions for normal operation. Region 1 is a control region before cut-in wind speed where the wind is used for rotor start-up and the generator toque is zero. Region 2 is a control region between cut-in and rated wind speed for optimizing power capture where a constant tip-speed ratio is maintained and the generator torque control is used. Region 3 is a control region above the rated wind speed where the generator torque or the power is held constant and the blade pitch control is used. There are two more linear transitional regions: Region 1½ and Region 2½ placed between Region 1 and 2 and Region 2 and 3 respectively, which allows the machine to reach rated torque at rated speed [27,28].

The mechanical power P_a gained by the rotor is given as [29],

$$P_a = \frac{1}{2}\rho\pi R^2 V_r^3 C_P(\lambda,\beta) \tag{1}$$

where ρ is the air density, R is the rotor radius, V_r is the effective wind speed on the rotor, C_p is power efficiency coefficient. Similarly, the wind induced thrust fore acting on the rotor plane causing a fore-aft motion is given as Eq. 2,

$$F_t = \frac{1}{2}\rho\pi R^2 V_r^2 C_T(\lambda,\beta) \tag{2}$$

The coefficients C_P and C_T are both functions of tip-speed-ratio (TSR) λ and blade pitch angle β. TRS is defined as the ratio between the rotor speed and wind speed,

$$\lambda = \frac{\omega_r R}{v_r} \tag{3}$$

where ω_r is the rotor angular rotational speed, v_r is the wind speed.

The aerodynamic torque of the rotor T_a can be defined as the ratio between the rotor power P_a and the rotor angular rotational speed ω_r as,

$$T_a = \frac{P_a}{\omega_r} \tag{4}$$

In Region 2, the optimum TSR is maintained, thus Eq.3 is simple. The generator torque is varied as the square of the rotor speed:

$$T_a = \frac{1}{2}\rho\pi R^5 \omega_r^2 \frac{C_{P\max}}{(\lambda_{opt})^3} \tag{5}$$

where, $C_{P\max}$ is the maximum power coefficient, corresponding to optimum TSR λ_{opt} at a particular blade pitch angle ($\beta = 0^\circ$).

The complete nonlinear aeroelastic wind turbine model can be linearized by FAST by developing state matrices of a wind turbine 'plant' to aid in controls design and analysis. The complete nonlinear aeroelastic equations of motion as modeled in FAST is written as follows [28,29]:

$$M(q,u,t)\ddot{q} + f(q,\dot{q},u,u_d,t) = 0 \quad (6)$$

where M is the mass matrix, f is the nonlinear "forcing function" vector, q is the vector of displacements, $\dot{q}$ and $\ddot{q}$ are the velocities and accelerations, u is the vector of control inputs, u_d is the vector of wind input 'disturbances', and t is time.

FAST numerically linearizes the aeroelastic equations of motion by perturbing each of the system variables about their respective operating point values. Expanding the equations of motion as a Taylor series approximation results in the second-order linearized representation of the equations:

$$\tilde{M}\ddot{q} + \tilde{C}\dot{q} + \tilde{K}q = \tilde{F}u + \tilde{F}_d u_d \quad (7)$$

where $\tilde{M}$, $\tilde{C}$, $\tilde{K}$ are the linearized mass matrix, damping matrix and stiffness matrix; $\tilde{F}$ is the control input matrix and $\tilde{F}_d$ is the wind input disturbance matrix.

2.3 Negative damping

With a conventional variable-speed, variable blade-pitch-to-feather control system, the steady state thrust force is reduced with the increasing wind speed in Region 3 (over rated). This effect may induce negative damping in the system that may lead to large resonant motions of floating wind turbine [6,18-20]. More specifically, the nacelle of the wind turbine in operation will oscillate forward and backward at above rated wind speed. The relative wind speed experienced by the blade is slightly higher when it is moving forward and this leads to a faster rotor speed. As a result, the blade pitch angle will increase to reduce the attack angle and then the rotor speed. The decreased thrust force then causes the nacelle to move more forwards [19]. Similar case be seen when the nacelle moves backwards.

This negative damping is less of a problem with fixed foundations because the system lowest eigen frequency is the tower fist fore-aft frequency. While the lowest natural frequencies decrease significantly when turbine is mounted on the floating foundation. Typically, it is an order of magnitude lower than that of the tower [19]. Some stability problems could occur when a turbine with very low natural frequencies is regulated by a normal pitch controller [18]. The structure would vibrate with the controller's frequency especially for a larger size of wind turbine. To improve the response of the floating wind turbine system, it is a possible approach to increase damping in a specific mode to stabilized the motion. This can be achieved by tuning the conventional wind turbine controller with the proportional-integral (PI) gain schedules or applying unconventional control scenario such as the active stall control.

It is found that if simply detuning the controller by decreasing the PI gain parameters to limit the gains of the blade pitch angle, the generator speed will exceed the design rated speed causing severe blade damage. Therefore, in this paper, the DRC baseline controller is modified by keeping the damping ratio constant and changing the natural frequency of the controller to characterize and account for the response features. In addition, the active stall control method is tailored and compared with pitch-to-feather controller for this 10MW RWT with the proposed TLP foundation.

3. Control Methodology

3.1 DRC baseline controller

The Delft Research Controller (DRC) provides an open, modular, and fully adaptable baseline wind turbine controller to the scientific community [21]. This new controller can be applied to the existing reference wind turbines by simulation software such as FAST, Bladed or HAWC which uses the bladed-style DISCON controller interface. In this way, systematic assessments, comparisons, and different control strategies can be realized. The complied controller is configured by a single control setting parameter file which removes the need for repetitive recompilation of the source code under a single change in control settings. Thus, users can collaborate the controller directly in the parameter file for each wind turbine model.

The DRC baseline controller implements torque and pitch controllers to enable the variable-speed variable-pitch control strategy. It also provides the individual pitch control (IPC) and the yaw-rate control strategies. The pitch and torque controllers use a generator speed measurement filtered by a second-order low-pass filter to calculate the error from the reference parameter. Both controllers act on individual generator speed set points: VS_RefSpd for torque control and PC_RefSpd for pitch control, as shown in Fig.3. The controllers continuously calculate the below-rated (GenBrTq) and above-rated (GenArTq) torque references. In Region 3 above rated operation, two strategies can be chosen to be either in constant power mode or constant torque mode. All variables regarding torque control are indicated by their respective names present in the control parameter file.

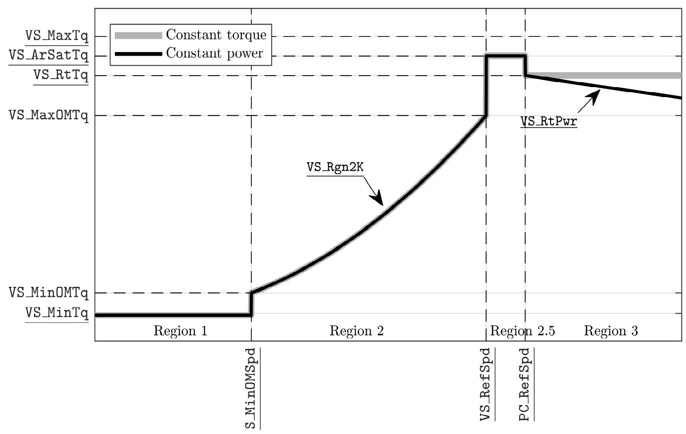

Fig. 3. Torque control strategies implemented in the DRC [21].

The gain-scheduled proportional-integral (PI) control system is widely adopted as a baseline controller and is used in Region 3 to compute the collective blade pitch angle. The PI gains are scheduled on the commanded pitch angle of the previous controller iteration. The form of the gain scheduled proportional integral control can be written as follows:

$$\Delta\theta = GS(\theta)(K_P\Delta\omega + K_I\int_0^t \Delta\omega) \tag{8}$$

where $\Delta\theta$ is the small perturbation of the blade pitch angle around the operation point, $\Delta\omega$ is the error between the measured rotor speed and the rated set point value, and K_P, K_I are the proportional and integral gains tuned at the operating points. The dimensionless gain correction factor $GS(\theta)$ is depended on the blade-pitch angle [25]:

$$GS(\theta) = \frac{1}{1+\theta/\theta_K} \tag{9}$$

where θ_K is the blade-pitch angle at which the pitch sensitivity has doubled from its value at the rated operating point.

3.2 PI gain schedule

As mentioned, the baseline pitch controller is implemented as a gain-scheduled PI-controller. The perturbation of the blade pitch angle can be computed by choosing appropriate PI gains (K_P, K_I) which are scheduled on the commanded pitch angle of the previous controller iteration. In Refs. [6, 24], a series of derivations were conducted to compute these object-based gains which can be expressed once the sensitivity of aerodynamic power to rotor collective blade pitch $\partial P/\partial\theta$ is known:

$$K_P = \frac{2I_{Drivetrain}\Omega_0\zeta_\varphi\omega_{\varphi n}}{N_{gear}(-\partial P/\partial\theta)} \tag{10}$$

$$K_I = \frac{I_{Drivetrain}\Omega_0 \omega_{\varphi n}^2}{N_{gear}(-\partial P / \partial \theta)} \tag{11}$$

where $I_{Drivetrain}$ is the drivetrain inertia cast to the low-speed shaft, Ω_0 is the rated rotational speed, $\omega_{\varphi n}$ is the natural frequency of the controller, ζ_φ is the damping ratio, N_{gear} is the gearbox ratio.

The aerodynamic property of the rotor $\partial P / \partial \theta$ which depends on the wind speed, the rotor speed, and the blade pitch angle. It is obtained by a linearization analysis about the rotor collective pitch angle perturbation at each operating point and calculating the variation in aerodynamic power [24]. This allows to design the control parameters in a way that the total systems behave as desired with input of damped natural frequency and damping ratio [25].

The instability problems could occur when turbines with very low natural frequencies and combined with a traditional pitch controller. It is influenced by the thrust force on the tower motion which has been explained as a contribution to the damping [18]. Compared to the motion of the tower, too fast pitch regulation can account for this low damping. Therefore, different natural frequency of the controller ($\omega_{\varphi n}$) is considered based on the gain schedule in DRC baseline controller. The rotor and the platform performances are investigated to access the controller. The revised PI gains are calculated in accordance with the Eqs. (10,11) based on the chosen natural frequencies and a recommended damping ratio of 0.7 [25]. The natural frequency of the DRC baseline controller $\omega_{\varphi n}$ (0.06 Hz) is then reduced to $\omega_{\varphi nb}$ 0.02 Hz (below) and increased to $\omega_{\varphi na}$ 0.10 Hz (above) as comparisons. In this way, the characteristics of the rotor and platform performances of the 10 MW offshore floating wind turbine influence by the control frequency are investigated.

3.3 Active stall control

The traditional variable speed controller leads to a reduction in rotor thrust force with increasing wind speed in Region 3, since it applies the blade-pitch-to-feather speed control regulation. However as has illustrated in Refs. [18,20,25,33], it is possible to regulate torque (or power) by pitching the blade the other way. This is opposite to the normal pitch control. With a high angle of attack, the drag and thrust force on the turbine increase, while the torque and power become more stable. This active stall control shows a good performance for both rotor and the platform which suggests an alternative method to solve the negative damping issue for a floating concept offshore wind turbine. Because of the drag force and thrust force increase as the increasing wind speed in overrated range, this active pitch-to-stall control may damp the platform motions more effectively. Although this method has been shown to be effective in simulation, it has not been widely pursued and investigated in industry given the uncertainty of the increased dynamic loads on turbine blades which might be a problem for structural design of blades [20,33].

This method has been tested for a 5MW floating barge concept in Refs. [6,24]. As suggested, the blade pitch angles are negative over the wind speed in Region 3. Likewise, the gain-scheduled PI control is implemented in the active-pitch-to-stall controller. The gain scheduling is less of a requirement because the variation of $\partial P / \partial \theta$ is less pronounced in Region 3, suggested by Refs. [20,24]. It also suggests that constant gains are possible in this schedule to be developed by using the values of $\partial P / \partial \theta$ in a middle wind speed in Region 3. While these gains applied in the stall controller are not constant but negative-valued gains from the baseline controller.

Apart from revising the PI gain parameters in DISCON.IN file, the maximum pitch angles should be set as 0 degree in the file. The recommended damping ratio (ζ_φ) of 0.7 is chosen and the control frequency ($\omega_{\varphi n}$) of 0.06 Hz is tuned. This revised control schedule is tested with the DTU 10 MW RWT and the rotor and platform performances are obtained and discussed in Section 4.

4 Results and Discussions

The influence of wind turbine control actions on the 10 MW TLP wind turbine is investigated in terms of the rotor and the platform performances. Different natural frequencies of the controller are considered by revising the gains at the operating points. Finally, the tailored active stall controller is compared with baseline controller and coupled effects are presented with respect to the rotor and platform performances.

The dynamic simulations are performed under two wind regimes. One is the uniform wind speed varying constantly from 4 m/s (cut-in) to 17 m/s (over-rated) with 500 s duration time for every increasement of 1 m/s in wind speed. The other is the turbulent wind speed 17 m/s with 20% turbulence intensity. For the turbulent wind condition, the incident wave is considered and compared with the still water condition.

4.1 DRC baseline controller

First the performance of the DRC baseline controller ($\omega_{\varphi n}$=0.06 Hz) with a land-based foundation and a floating platform foundation is shown in Fig. 4. A wind step case from 4 m/s to 25 m/s is chosen and for each wind step in overrated region, a time duration of 500s is adopted to stabilize the system.

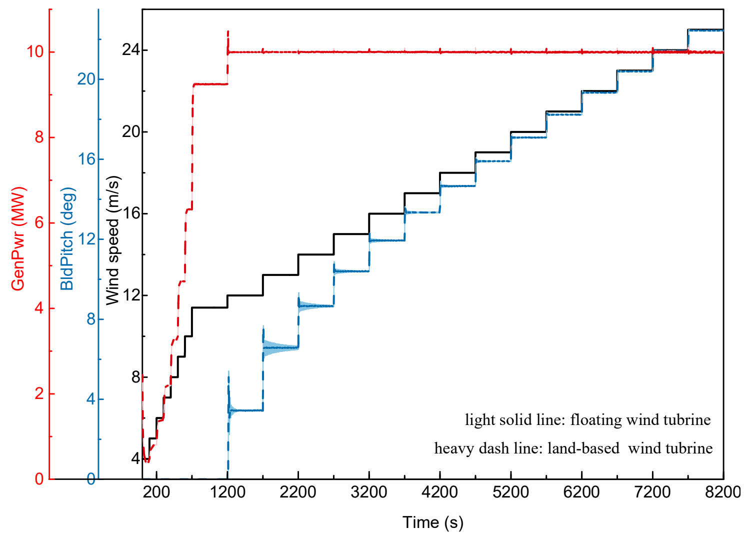

Fig. 4. DRC: black line: wind speed, blue line: blade pitch angle, red line: generator power.

Fig. 4 presents wind steps (black line), blade pitch angle (blue line) and generator power (red line) time series under the control frequency of 0.06 Hz by DRC baseline controller. Two boundary conditions are considered: the onshore land-based foundation and the offshore floating foundation. The boundary condition of land-based foundation is achieved by disabling the six degrees of freedom of the TLP platform, and the result is drawn in heavy dash line in Fig. 4. The blade pitch angle and the generator power under these two boundary conditions are compared. For the land-based foundation, the controller performs well as the wind speed increases and the rotor speed and the power generation promptly become stable about 9.6 RPM and 10 MW respectively after wind speed reaching the rated wind speed (11.4 m/s). However, the blade pitch angle shows a clear fluctuation for the floating foundation because of the reduction of the system stiffness. This also suggests that the PI gains tuned for reference wind turbines should consider the supporting structure to moderate the fluctuation of the blade pitch angle. For instance, the proportional term in the original gain schedule may need to be decreased when it is applied to a floating foundation.

4.2 DRC baseline controller – with different control frequencies

The DRC baseline controller adopts a natural frequency $\omega_{\varphi n}$ of 0.06 Hz and a damping ratio of 0.7 for DTU 10 MW RWT. As has been explained, two more control frequencies ($\omega_{\varphi nb}$=0.02 Hz and $\omega_{\varphi na}$=0.10 Hz) are selected as comparisons with the same damping ratio. The lower control frequency $\omega_{\varphi nb}$ is taken considering that the natural frequency of this floating wind turbine system in surge mode is 0.042 Hz. Besides, it is recommended to adopt a control frequency of 0.6 rad/s (about 0.10 Hz) which is also higher than that applied in the baseline controller ($\omega_{\varphi n}$). It is unnecessary to consider even faster control frequencies given that the pitch natural frequency is much larger.

The system responses of floating wind turbine under three control frequencies ($\omega_{\varphi nb}$, $\omega_{\varphi n}$, $\omega_{\varphi na}$) are presented in terms of a uniform stepwise increasing wind range and a turbulent wind speed shown in Fig. 5 and Fig. 6. The wind step case is from 4 m/s to 17 m/s. The time duration for wind speed below the rated speed is 100s and 500s for these above the rated speed.

4.2.1 Uniform wind speed - Rotor performance

Fig. 5 depicts the rotor performances which include the blade pitch angle (BldPitch), the rotor speed (RotSpeed) and the generator power (GenPwr). The rotor thrust force (RotThrust) and the induced tower top fore-aft motion (TTDspFA) are also depicted.

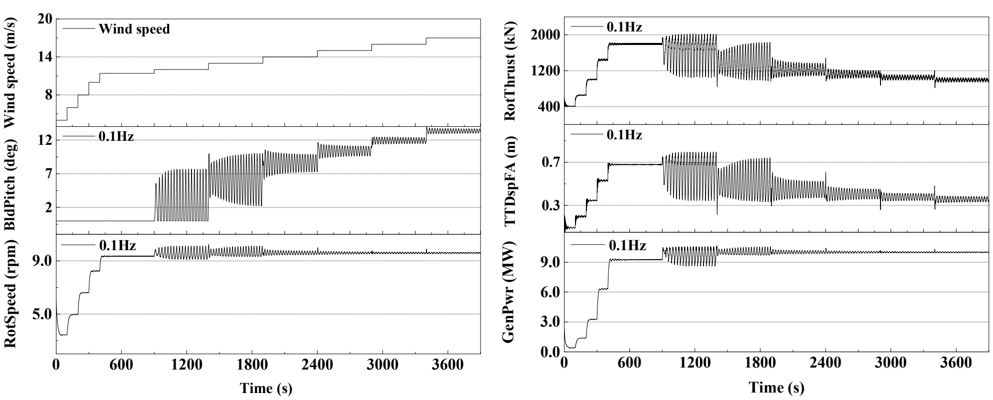

$\omega_{\varphi na}$ = 0.10 Hz (above the reference control frequency)

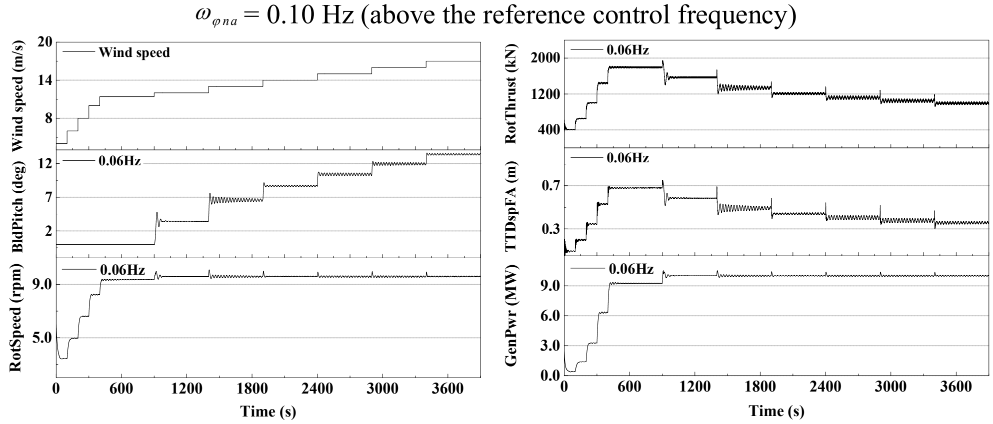

$\omega_{\varphi n}$ = 0.06 Hz (reference control frequency)

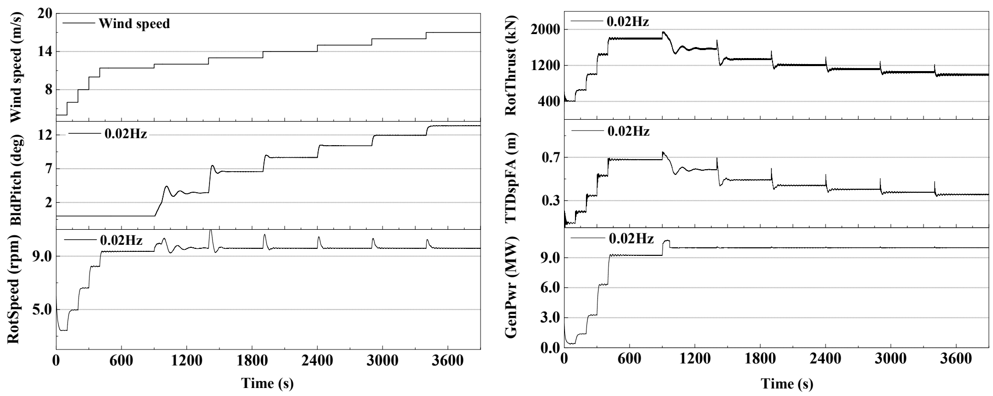

$\omega_{\varphi nb}$ = 0.02Hz (below the reference control frequency)

Fig. 5. Different rotor step response depending on the control natural frequencies.

It was found that the control frequencies $\omega_{\varphi nb}$ and $\omega_{\varphi n}$ both have superior performance. The fastest control frequency corresponds to the most fluctuations in blade pitch and thrust force which further leads to a larger tower top motion especially for these wind speed at the start of the overrated region. With higher wind speed, the control natural frequency induced differences begin to fade. Distinct fluctuation in blade pitch accounts for the variation of the thrust force and the further tower top motion. The top motion can influence the relative wind speed experienced by the wind turbine which in return affect the thrust force. Generally, rotor speed and generator power are less sensitive to the change of control frequency. Even though the 1st tower fore-aft (bending) mode has a natural frequency of 0.25 Hz which is much higher than all of three control frequencies, the control frequency induced effect at tower top motion is still clear.

4.2.2 Uniform wind speed - TLP Platform performance

The TLP platform performances under different control frequencies are illustrated in Fig. 6 in terms of surge, pitch, and yaw responses. These three modes are chosen because the foundation is symmetric in surge direction and there is no incident wave involved in.

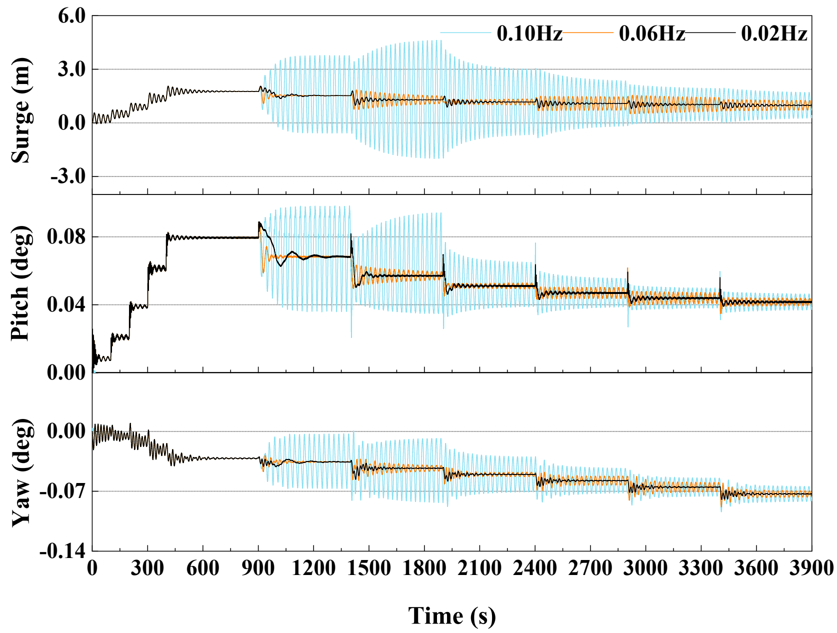

Fig. 6. Different platform motion step responses depending on the control natural frequencies ($\omega_{\varphi na}$, $\omega_{\varphi n}$, $\omega_{\varphi nb}$).

From Fig. 6, it is found that the control frequency $\omega_{\varphi n}$ and $\omega_{\varphi nb}$ are better in platform motion performances. The gentlest fluctuation occurs with the lowest control frequency $\omega_{\varphi nb}$ which also takes longer time to stabilize the motion. Clear and dramatic fluctuations can be seen once reaching the rated wind speed especially for the control frequency $\omega_{\varphi na}$ (0.10 Hz). The surge, pitch and yaw motions become more stable with higher wind speed, which follows the trend of thrust force. Since there is no wave involved in, the induced platform motions are generally small. The differences between the control frequencies $\omega_{\varphi n}$ and $\omega_{\varphi nb}$ are also small. Considering that the platform has a natural frequency of 0.04 Hz in surge mode which is larger than control frequency $\omega_{\varphi nb}$ (0.02 Hz), the surge motion is more stable with $\omega_{\varphi nb}$, which agrees with Ref [18].

However, it is not the case in pitch mode because the natural frequency in pitch mode is higher than $\omega_{\varphi na}$, $\omega_{\varphi n}$, and $\omega_{\varphi nb}$. Because the pitch motion is coupled with and dominated by the surge motion, as a result, it prompts the low frequency effect. With the baseline control frequency, both pitch and yaw motions can be stabilized swiftly. Overall, the mean values of motions are not influenced by the controller's natural frequency.

4.2.3 Turbulent wind speed

The control frequency induced responses for rotor and platform motions are compared under turbulent wind condition. The mean wind speed is 17 m/s with 20% turbulent intensity generated by TurbSim [33]. As mentioned, the hydrodynamic wave loads are considered to illustrate the negative damping issues. Two irregular wave conditions are selected with a significant wave height of 6 m, wave peak period of 10 s and a wave height of 9.14 m, wave peak period of 13.6 s, respectively. The turbulent wind and wave elevations are shown in Fig. 7. The simulations time is 3600 s in total and results in Fig. 8 and 9 are shown within a period from 2500 s to 3000 s for clarity. The still water condition is depicted in Fig.8. The rotor and platform performances under coupled wind and wave conditions are illustrated by the case of 9.14 m wave height only in Fig.9.

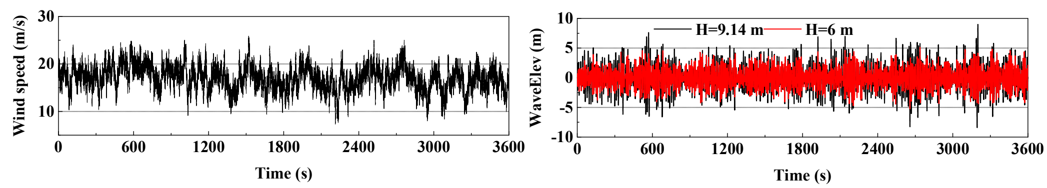

Fig. 7. Turbulent wind and wave elevation time history series.

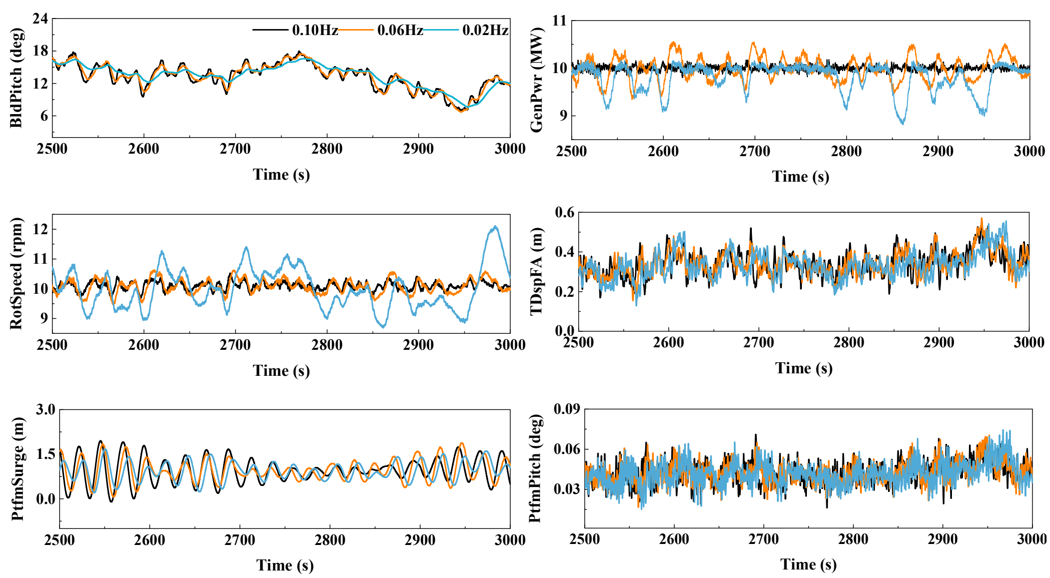

Fig. 8. Rotor and platform performances under different control frequencies at 17 m/s turbulence wind and still water.

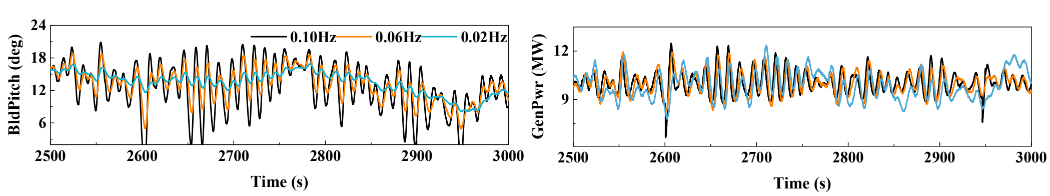

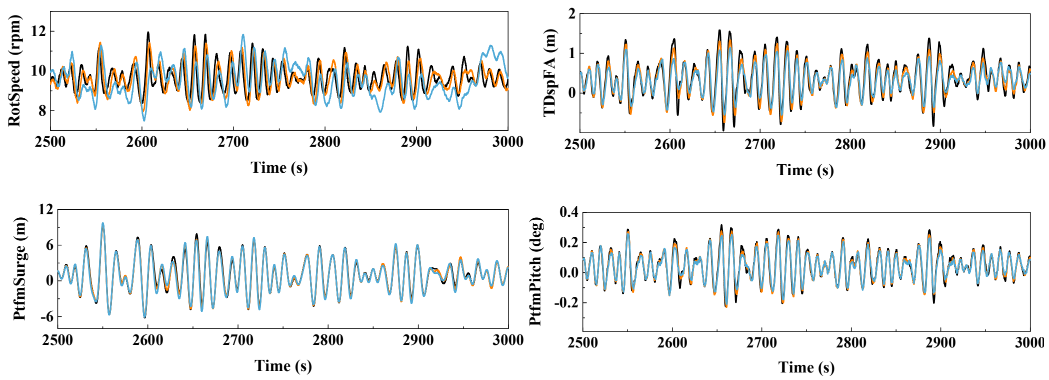

Fig. 9. Rotor and platform performances under different control frequencies at 17 m/s turbulence wind and irregular wave (significant wave height 9.14 m).

In Fig. 8 and Fig. 9 the blade pitch angle, generator power, rotor speed and tower top motion variations are shown with respect to different control frequencies. The variations of blade pitch angle and rotor speed under control frequency of $\omega_{\varphi n}$ (0.06 Hz) and $\omega_{\varphi na}$ (0.1 Hz) are quite consistent. While rotor speed with control frequency $\omega_{\varphi nb}$ (0.02 Hz) fluctuates more significantly, which is quite different from the blade pitch angle. Blade pitch angle shows a significant difference resulting from the control frequency with irregular wave. As for the tower top motion, the control frequency induced difference is quite limited in still water but clearer when hydrodynamic wave is involved. The reason for slow variations in blade pitch and rotor speed with faster control frequency is because the blade can response quickly to varying wind speeds and keep the relative wind speed stable. As a result, the power output is more stable. While this change exerts less influence on the tower top motion since the natural frequency of 1st tower bending mode is much higher than the control frequency. When the wave load is considered, the overall tower top motion and platform pitch are larger and obvious deviations in amplitude can be seen due to the control frequency.

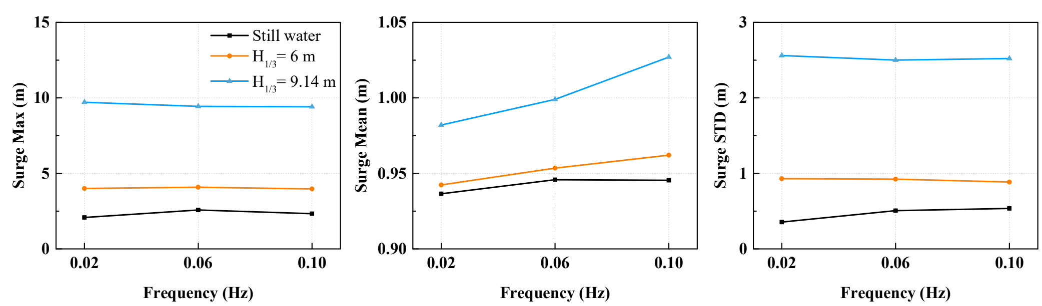

Fig. 10. Maximum values, mean values, and standard deviations of the platform motions in surge mode vs. different control frequencies at 17 m/s turbulence wind and irregular wave conditions.

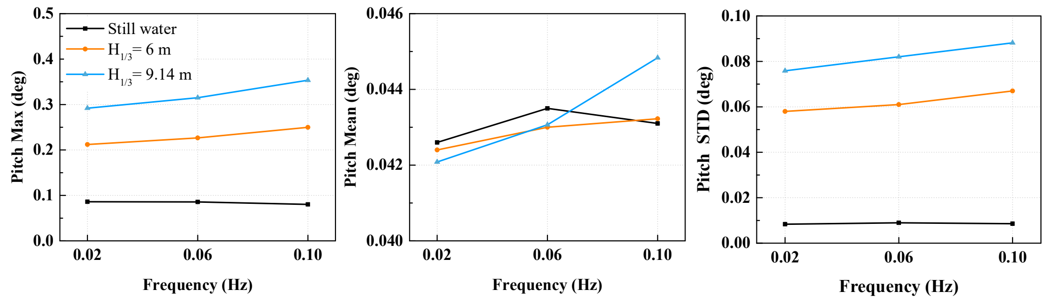

Fig. 11. Maximum values, mean values, and standard deviations of the platform motions in pitch mode vs. different control frequencies at 17 m/s turbulence wind and irregular wave conditions.

The statistic results of the platform surge and pitch motion responses to different control frequencies are compared in Fig.10 and Fig.11. As explained, the wave load case with 6 m wave height is not shown in time series but the motion statistics are categorized here to better illustrate the negative damping issue. It is found that in still water conditions the control frequency induced difference in platform motions are not obvious compared with the cases when wave loads are involved. The mean values of surge and pitch motions are increased by 5-6% with higher control frequency $\omega_{\varphi na}$ especially for the pitch motion. Large surge motions occurred in $\omega_{\varphi n}$ (0.06 Hz) and $\omega_{\varphi na}$ (0.1 Hz) is probably due to the lower surge natural frequency of the floating system (0.042 Hz) which is lower than the control frequencies. As for pitch mode, the natural frequency is higher than $\omega_{\varphi na}$, but the coupled effect of surge and pitch motions influence the pitch motion. Thus, with higher control frequency, pitch motion response is also magnified.

In general, the control frequencies involved with negative damping effects on the platform surge and pitch motions can be observed in coupled wind and wave conditions and it is clearer when the wave height is larger. Higher control frequency can lead to increases in surge and pitch motions.

4.3 Active stall control

4.3.1 Rotor performance

Active stall control strategy (pitch-to-stall) is opposite to the normal pitch control for the blade is pitched to a high angle of attack, the stall condition, thus the lift force decreases as well as the rotor speed. The system responses are shown in Fig. 12 and Fig. 13 within Region 3 (overrated wind speed). The simulations are conducted with uniform wind speed varying from 11 m/s to 25 m/s with a duration time of 500 s for every increasement of 1 m/s in wind speed.

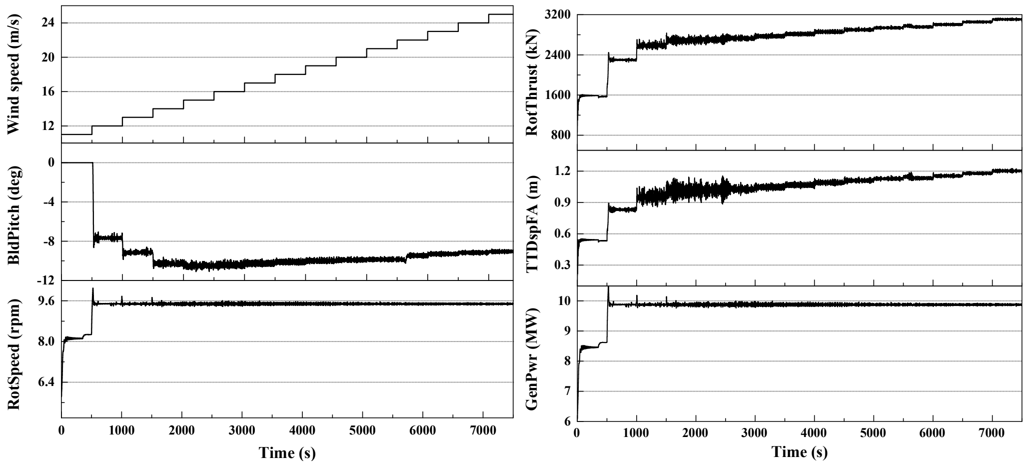

Fig. 12. Different rotor step response with active stall control.

In Fig. 12, the wind steps, blade pitch angle, rotor speed, thrust force, tower top motion and generator power are depicted. In general, the active stall controller works well and the rotor responses are fine. The blade pitch angle decreases rapidly at first before reaching a value around negative 11 degree and then it basically maintains stable with a slight growth as the wind speed goes up. The rotor speed experiences the most growth early and then it tends to level off at the rated speed (9.6 RPM). The same trend can be seen in the generator power. The rotor thrust force increases in stages at first and then keeps a slow and steady increasing trend. The same trend is observed in tower top motions because it follows the thrust force. This ascending trend is different from that with the pitch-to-feather controller in which the rotor thrust force decreases, and in this way the negative damping can be avoided.

4.3.2 Platform performance

The platform performances with the pitch-to-stall controller are shown in Fig. 13. Similarly, the surge, pitch and yaw modes are chosen.

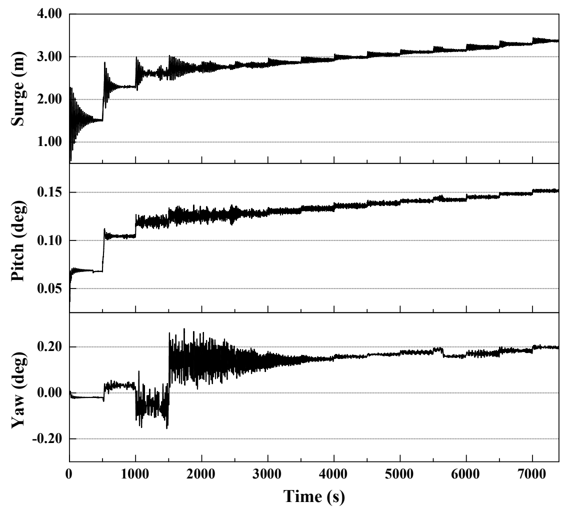

Fig. 13. Different platform step responses with active stall control.

As can be seen, the total responses are stable, but significant fluctuation occurs at the first stages of the wind speed growth (below 14m/s). The platform motions become stable and less fluctuating for higher wind speed. The surge and pitch motions are larger compared with these values shown in Fig. 6 with the baseline controller, under the same wind speed especially in pitch mode. This can be accounted for by the increasing thrust force in Region 3 with active stall control method. Unlike surge and pitch motions showing stepwise increases at first, there is a slight growth followed by a clear decrease in yaw mode, before it finally shows a significant increase. The platform has a mean positive yaw motion, which is opposite to the baseline controller where a negative yaw motion occurs. Given that the system is symmetric and the wind speed is uniform in surge direction, the yaw motion should oscillate around the original equilibrium position. However, it fluctuates drastically and reaches to a positive deviation at the start of the Region 3. The reason for these yaw deviations in opposite directions by the baseline controller and the pitch-to-stall controller cannot be explained yet based on above analyses.

Overall, the wind turbine system shows reasonable rotor and platform motion responses by the active stall controller especially for power generation. Except that the thrust force is much larger in overrated region which may become a problem for the safety of these long slender blades. Even though, this could very well be a feasible solution for floating wind turbines not only for 5 MW size, but also for 10 MW size [28].

4.4 Pitch-to-feather and pitch-to-stall

The conventional approach for controlling wind turbines is pitching the blade to feather in high wind speed region. This pitch-to-feather control strategy, applied in DRC baseline controller, is compared with the pitch-to-stall control strategy with respect to the rotor and platform performances under the turbulent wind condition in still water and irregular wave condition as shown in Fig. 14-19. The mean wind speed is 17 m/s with 20% turbulent intensity. The irregular wave condition has a significant wave height of 9.14 m and peak period of 13.6 s. The entire simulation time is 3600 s.

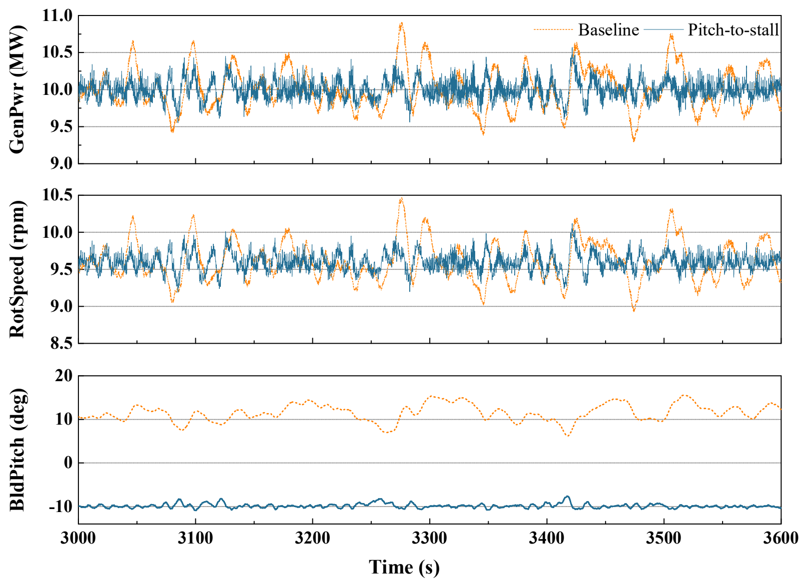

Fig. 14. Comparison of rotor performances at 17 m/s turbulence wind and still water condition with the baseline controller and the pitch-to-stall controller.

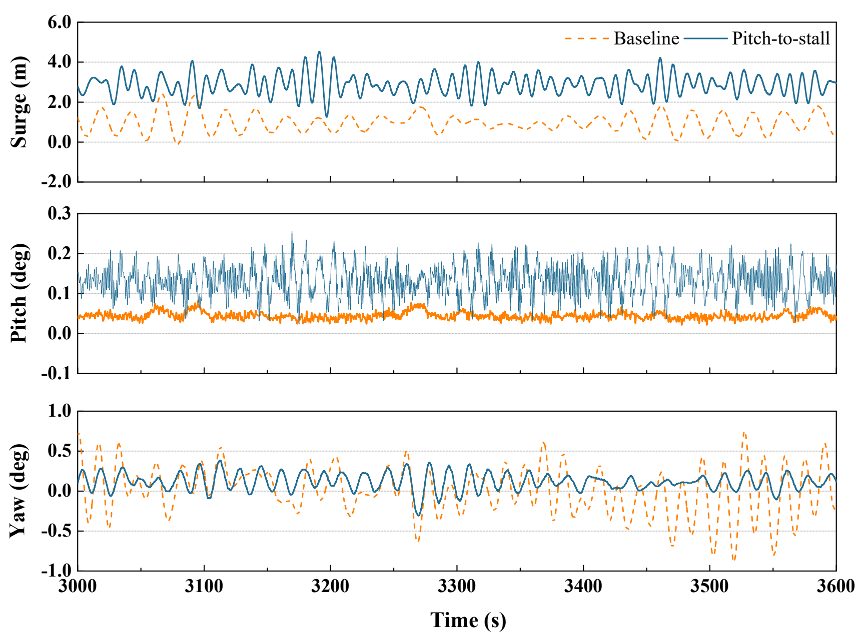

Fig. 15. Comparison of platform performances at 17 m/s turbulence wind and still water

condition with the baseline controller and the pitch-to-stall controller.

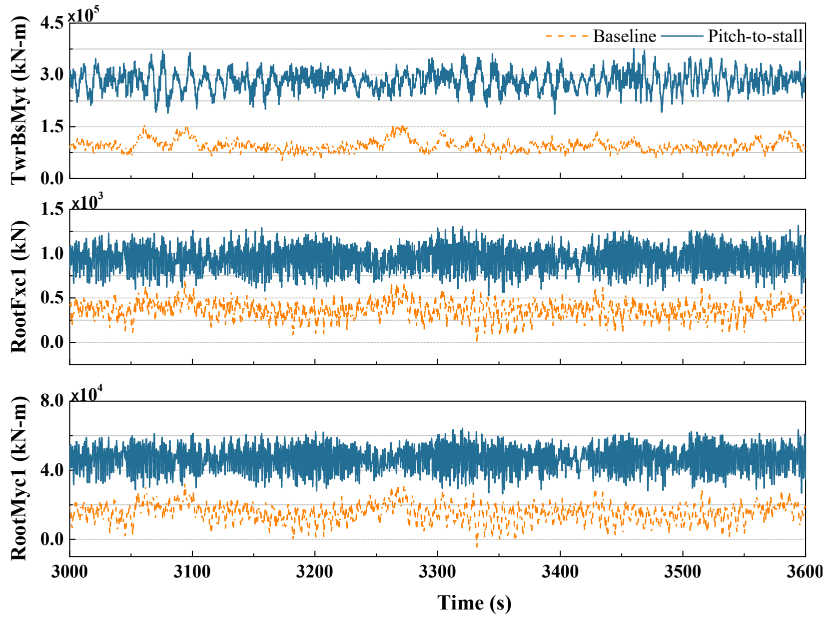

Fig. 16. Comparison of tower base moment, blade root axial force, and blade root bending moment at 17 m/s turbulence wind and still water condition with the baseline controller and the pitch-to-stall controller.

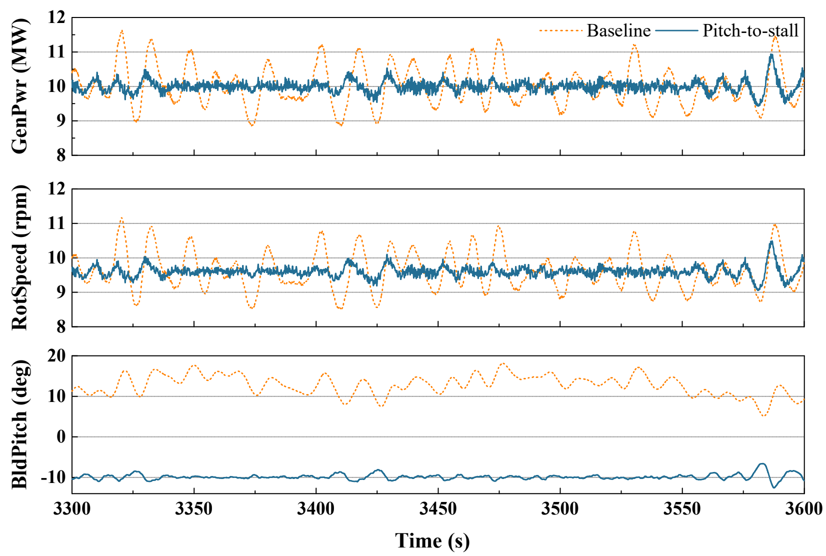

Fig. 17. Comparison of rotor performances at 17 m/s turbulence wind and irregular wave condition with the baseline controller and the pitch-to-stall controller.

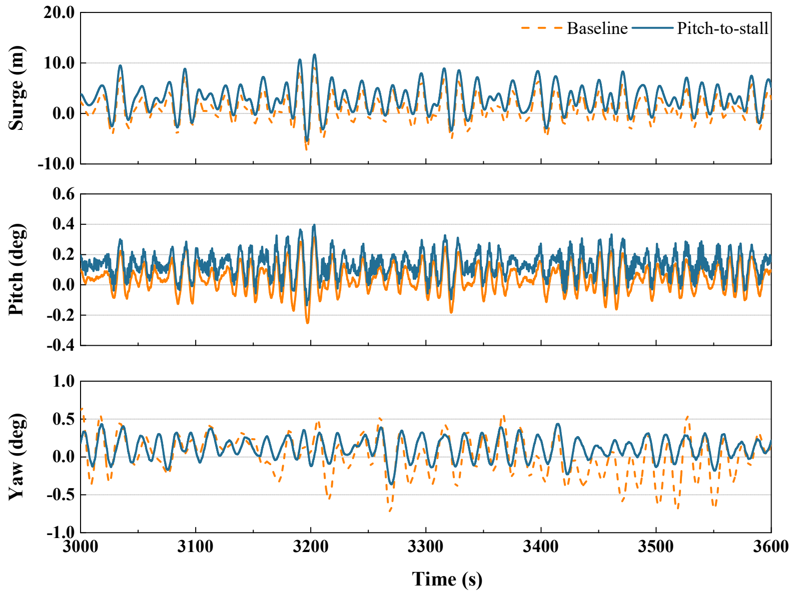

Fig. 18. Comparison of platform performances at 17 m/s turbulence wind and irregular wave condition with the baseline controller and the pitch-to-stall controller.

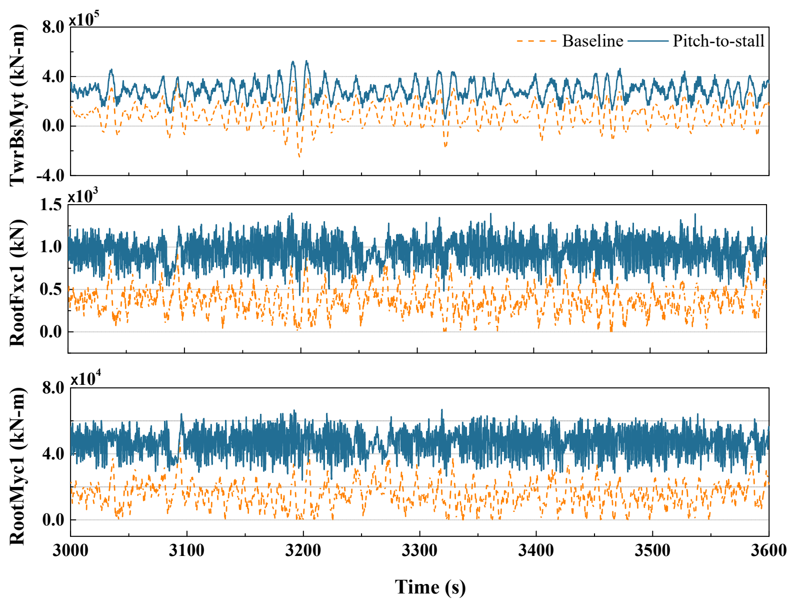

Fig. 19. Comparison of tower base moment, blade root axial force, and blade root bending moment at 17 m/s turbulence wind and irregular wave condition with the baseline controller and the pitch-to-stall controller.

As shown in Fig. 14 and Fig. 17, the generator power is regulated well by both controllers, and less fluctuations of the rotor speed and the blade pitch angle indicate that active blade-pitch-to-stall controller performs even better than the baseline controller. However, this is not the case when it comes to the platform motions. As depicted in Fig. 15 and Fig. 18, the controller induced effects are more evident. In surge and pitch modes, with the baseline controller, the mean values are smaller and variations are more stable which is much clear in still water condition. But in yaw mode, the mean yaw angle is positive for pitch-to-stall controller and negative for baseline controller which also exerts larger fluctuation.

Figure 16 and 19 depict the tower base bending moment and the blade root force and moment with respect to baseline and active stall controllers. The baseline controller seems more sensitive to the wave load than pitch-to-stall controller based on the obvious fluctuations in Fig. 19. It is also found that these wind-induced forces are much larger in pitch-to-stall controller which is approximately twice higher than baseline controller. These large forces in pitch-to-stall controller may cause severe damage on rotor blades and the tower.

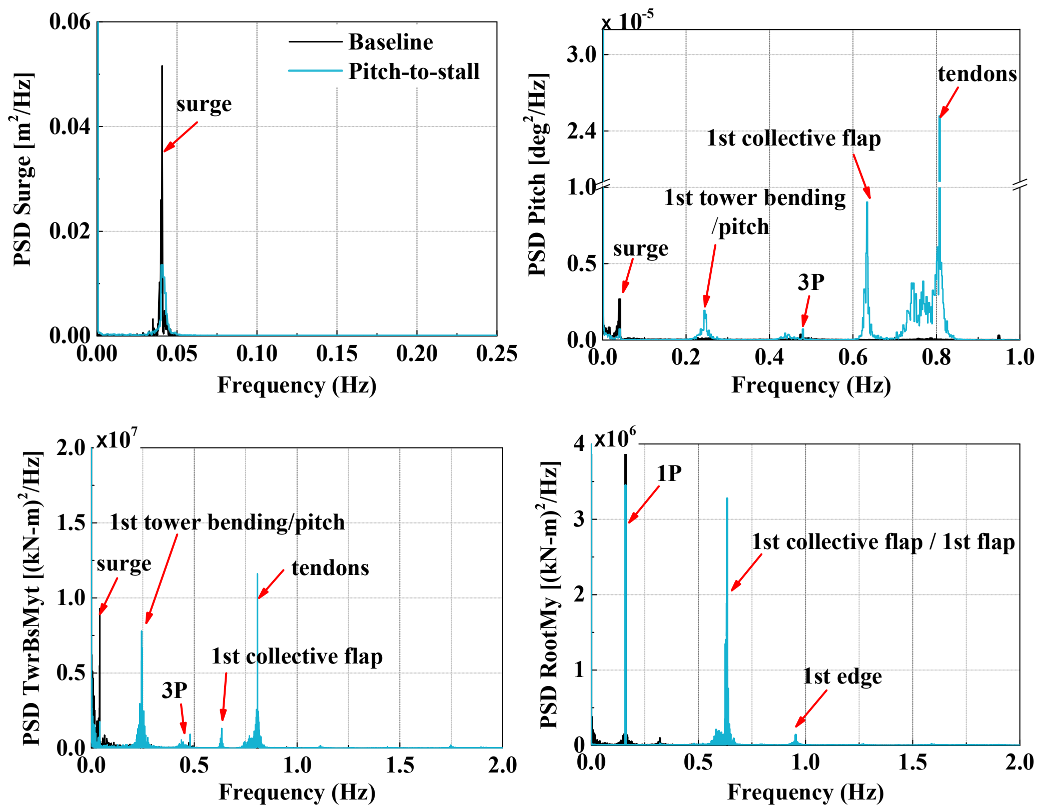

Fig. 20. Power spectra of surge motion, pitch motion, tower base bending moment, and blade root bending moment at 17 m/s turbulence wind and still water condition with the baseline controller and the pitch-to-stall controller.

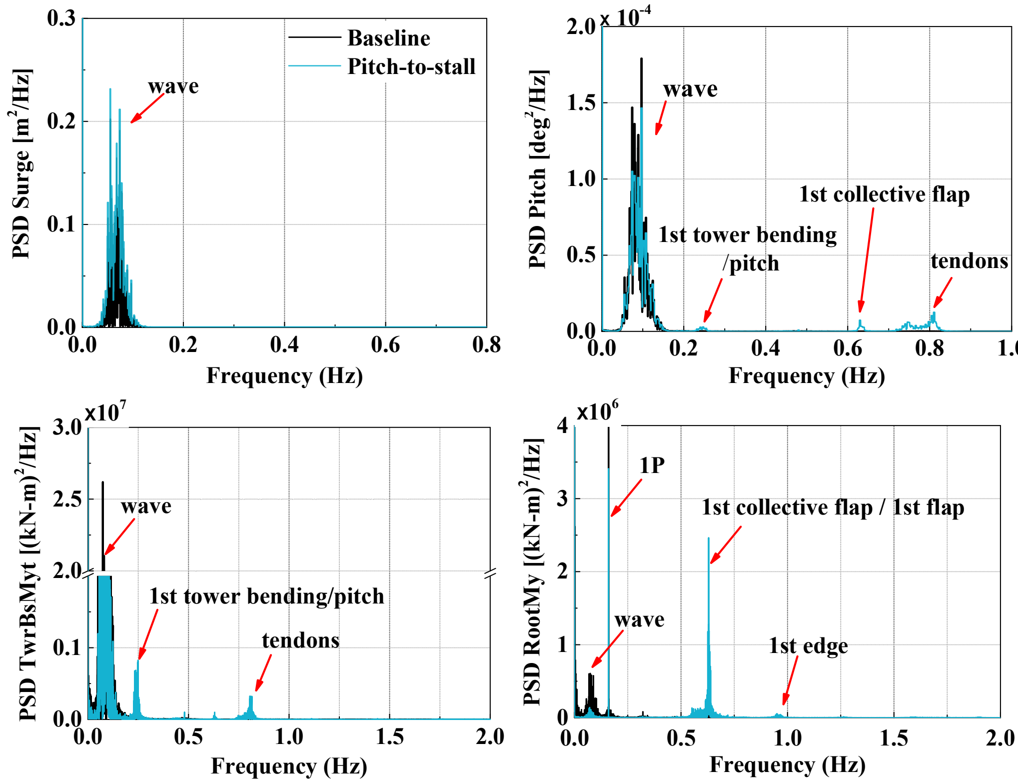

Fig. 21. Power spectra of surge motion, pitch motion, tower base bending moment, and blade root bending moment at 17 m/s turbulence wind and irregular wave condition with the baseline controller and the pitch-to-stall controller.

The power spectrum analysis is used to illustrate the controller induced effects on the variations of rotor, tower, and platform motions, as demonstrated in Fig. 20 and Fig. 21. The baseline controller and the pitch-to-stall controller show significant distinctions for resonant response in pitch motion, tower base and blade root bending moment. The pitch-to-stall controller can induce high frequency resonant responses in pitch mode such as 3P resonance response, 1st collective flap resonance response and even the contribution from the TLP tendons, which is obvious in still water condition. Visible high frequency resonance responses also can be seen in irregular wave condition for pitch-to-stall controller. The main reason is that the wind induced thrust force is much larger with pitch-to-stall controller which exaggerates the deformation of the blades and tower. The research work of Goupee [35] and Souza et al. [36] provides more various scenarios about the controller induced differences on the dynamic behavior of the floating wind turbine which can be combined with what has been shown in this paper as references.

The active stall controller shows better performances with respect to the blade pitch angle, rotor speed, and power generation; however, the platform motions and wind-induced structure forces are exaggerated with it. This agrees with the results in Ref. [30] that the pitch motion for the NREL 5 MW wind turbine is also larger with pitch-to-stall controller. But this does not contradict to the explanation of the negative damping issues by the pitch-to-stall controller. As illustrated in Ref [16, 28, 30], the steady thrust force in Region 3 with a normal controller is reduced as the wind speed increases which may introduce negative damping in the system and further lead to large resonant motion for floating wind turbine. On the contrary, it suggests that the baseline controller has an effective pitch damping ratio higher than that of the pitch-to-stall controller. Given that the control frequency adopted in the baseline and the active stall controllers is $\omega_{\varphi n}$ (0.06 Hz), this effective pitch damping effect is not prominent in Fig. 18.

5 Conclusions

This paper introduces the DRC baseline controller to evaluate the control strategies induced effects on the DTU 10 MW RWT with a floating TLP foundation. This open and adaptable baseline controller is implemented by using the FAST simulator to perform fully coupled dynamic analyses. The full-field wind flow is provided by TurbSim. Control frequency induced effects and dynamic responses of the DTU 10 MW floating wind turbine system are analyzed with the conventional blade-pitch-to-feather and active pitch-to-stall strategies considered. The baseline controller is tailored based on the PI gain schedule to obtain different control frequencies and to achieve the active stall control. This DRC baseline controller proves to be adaptable for large scale offshore wind turbines and can be collaborated and detuned by new control algorithms for further improvement.

The baseline controller regulates the 10 MW wind turbine well with control frequency $\omega_{\varphi nb}$ and $\omega_{\varphi n}$ for all wind speed conditions. While the control frequency can induce instability of the system within wind speeds below 15 m/s. The rotor responses perform better with and since the blade pitch angle changes slowly, which further leads to dramatically less fluctuations in thrust force and tower top motion, whereas the maximum rotor speed can be 10% larger due to this slow change. Generator power shows the least sensitivity to the control frequencies under uniform wind speed. The higher control frequency induced instability decreases rapidly with the increase of wind speed between 12m/s and 15m/s.

For turbulent wind speed, the blade pitch angle shows a slow variation with lower control frequency, which further leads to drastic fluctuations in rotor speed and generator power. Since high turbulent wind speed is taken, the generator power, rotor speed, and tower top motion are more stable with $\omega_{\varphi n}$ and $\omega_{\varphi na}$. Obvious deviations in motion response due to the control frequency can be seen when hydrodynamic wave load is considered. The fast control frequency involved with negative damping effect on platform surge and pitch motions are found in coupled wind and wave conditions.

As for the comparison of the active stall controller with the baseline controller, within uniform wind field, the rotor behavior with active stall controller is fine but the maximum platform motions are about twice as that of the baseline controller. With the same control frequency and turbulence wind condition, pitch-to-stall controller is better than baseline controller given the blade performances. However, in views of platform motions and wind-induced structural forces, the baseline controller is much better. The baseline controller seems more sensitive to the wave load than pitch-to-stall controller. Moreover, the power spectral analyses of motions and structural forces suggest that pitch-to-stall controller can lead to resonance responses of motion and forces in a wide range of frequency.

The control strategies investigated in this paper are based on DTU 10MW TLP floating foundation by using the DRC in corporation with FAST code, which provides a convenient method to modify and assess the control algorithms. It is also applicable to offshore wind turbines with other types of floating foundations. The research work proves the possibility of controlling a baseline wind turbine through different strategies by DRC. Further investigations should be done to better understand the control frequency induced dynamic effects on the floating wind turbine structures and system motions for the purpose of practical application.

ACKNOWLEDGMENTS

The authors would like to acknowledge the support from the National Natural Science Foundation of China (Grant Nos. 51679163 & 51779171), Tianjin Municipal Natural Science Foundation (Grant No. 18JCYBJC22800) and State Key Laboratory of Hydraulic Engineering Simulation and Safety (HESS-1602).

References

[1] Lee, J., Zhao, F. GWEG. Global Wind Report. Global Wind Energy Council. 2020.

[2] Moan T, Gao Z, Bachynski EE, Nejad AR. Recent advances in integrated response analysis

of floating wind turbines in a reliability perspective. Journal of Offshore Mechanics and Arctic Engineering, 2020,142.5..

[3] Jonkman, J.M., Matha, D., Dynamics of offshore floating wind turbinesanalysis of three concepts. Wind Energy, (2011) 14(4), 557-569.

[4] Robertson, A., Jonkman, J., Masciola, M., Song, H., Goupee, A., Coulling, A., Luan, C., Definition of the semisubmersible floating system for phase II of OC4 (No. NREL/TP-5000-60601). National Renewable Energy Lab. (NREL), Golden, CO (United1States). 2014.

[5] Casale, C., Lembo, E., Serri, L., Viani, S., Preliminary design of a floating wind turbine support structure and relevant system cost assessment. Wind Engineering, (2010) 34(1), 29-50.

[6] Jonkman J.M., Butterfield S., Musial W., Scott G. Definition of a 5-MW reference wind turbine for offshore system development, Technical report NREL-TP-500-38060, NREL, CO, USA. (2009).

[7]. C. Bak, F. Zahle, R. Bitsche, T. Kim, A. Yde, L.C. Henriksen, P.B. Andersen, A. Natarajan, M.H. Hansen, Design and performance of a 10 MW turbine, J. Wind Energy, (2013).

[8] Thomsen, K., Operation and control of large wind turbines and wind farms-design load basis, Risø-I-1967 (2003).

[9] Yuan, Y., Tang, J., On advanced control methods toward power capture and load mitigation in wind turbines. Engineering, (2017) 3(4), 494-503.

[10] Wright, A.D., Fingersh, L.J., Advanced control design for wind turbines; Part I: control design, implementation, and initial tests (No. NREL/TP-500-42437). National Renewable Energy Lab. (NREL), Golden, CO (United States) (2008).

[11] Hwas, A., Katebi, R., Wind turbine control using PI pitch angle controller. IFAC Proceedings Volumes, (2012) 45(3), 241-246.

[12] Lackner, M.A., An investigation of variable power collective pitch control for load mitigation of floating offshore wind turbines. Wind Energy, (2013) 16(4), 519-528.

[13] Lasheen, A., Elshafei, A.L., Wind-turbine collective-pitch control via a fuzzy predictive algorithm. Renewable Energy, (2016) 87, 298-306.

[14] Bossanyi, E.A., Individual blade pitch control for load reduction. Wind Energy: An International Journal for Progress and Applications in Wind Power Conversion Technology, (2003) 6(2), 119-128.

[15] Bossanyi, E. A., Further load reductions with individual pitch control. Wind Energy: An International Journal for Progress and Applications in Wind Power Conversion Technology, (2005) 8(4), 481-485.

[16] Selvam, K., Kanev, S., van Wingerden, J.W., van Engelen, T., Verhaegen, M., Feedback – feedforward individual pitch control for wind turbine load reduction. International Journal of Robust and Nonlinear Control: IFAC – Affiliated Journal, (2009) 19(1), 72-91.

[17] Li, F., Zhou, L., Li, L., Wang, H., Guo, H., Liang, Y., Individual Blade Pitch Control for Floating Wind Turbines Bearing the Coupling of Aerodynamic-Hydrodynamic–Mooring Loads. In 2019 22nd International Conference on Electrical Machines and Systems (ICEMS) (pp. 1-6). IEEE., 2019.

[18] Larsen, T.J., Hanson, T.D., A method to avoid negative damped low frequent tower vibrations for a floating, pitch controlled wind turbine. In Journal of Physics: Conference

Series (Vol. 75, No. 1, p. 012073). IOP Publishing, 2007.

[19] Van Der Veen, G.J., Couchman, I.J., Bowyer, R.O., Control of floating wind turbines. In 2012 American Control Conference (ACC) (pp. 3148-3153). IEEE, 2012.

[20] Jonkman, J. Influence of control on the pitch damping of a floating wind turbine. In 46th AIAA Aerospace Sciences Meeting and Exhibit, 2008. (p. 1306).

[21] Mulders, S.P. and van Wingerden, J.W., Delft Research Controller: an open-source and community-driven wind turbine baseline controller. Journal of Physics: Conference Series. Vol. 1037. No. 3. IOP Publishing, 2018.

[22] Hansen, M. H., Henriksen, L. C., Basic DTU wind energy controller. Wind Energy. DTU Wind Energy E, No. 0028, 2013.

[23] Hassan, G., Bladed User Manual. Garrad Hassan and Partners Limited Document, 2013.

[24] Jonkman, J. M., Dynamics modeling and loads analysis of an offshore floating wind turbine (No. NREL/TP-500-41958). National Renewable Energy Lab. (NREL), Golden, CO (United States), 2007.

[25] Hansen, M. H., Hansen, A., Larsen, T. J., Φye, S., Sørensen, Fuglsang, P., Control design for a pitch-regulated, variable-speed wind turbine, Risø-R-1500(EN), Roskilde, Denmark: Risø National Laboratory, January 2005.

[26] Emrah Kulunk. Aerodynamics of wind turbines, Fundamental and Advanced Topics in Wind Power, Dr. Rupp Carriveau (Ed.), ISBN: 978-953-307-508-2, InTech, Available from: http://www.intechopen.com/books/fundamental-and-advanced-topics-in-wind-power/aerodynamics-of-windturbines. (2011)

[27] Wright A D, Fingersh L J., Advanced control design for wind turbines. Part I: Control Design, Implementation, and Initial Tests, National Renewable Energy Lab., USA, 2008.

[28] Hansen, M. O., Aerodynamics of Wind Turbines, third Ed., Earthscan, USA, Routledge. 2015.

[29] Ebrahimi, F. M., Khayatiyan, A., Farjah, E., A novel optimizing power control strategy for centralized wind farm control system. Renewable energy, (2016) 86, 399-408.

[30] Ding, H., Han, Y., Zhang, P., Le, C., Liu, J., Dynamic analysis of a new type of floating platform for offshore wind turbine. In The 26th International Ocean and Polar Engineering Conference. International Society of Offshore and Polar Engineers, 2016.

[31] Ding, H., Han, Y., Le, C., Zhang, P., Dynamic analysis of a floating wind turbine in wet tows based on multi-body dynamics. Journal of Renewable and Sustainable Energy, (2017) 9(3), 033301.

[32] Han, Y., Le, C., Ding, H., Cheng, Z., Zhang, P., Stability and dynamic response analysis of a submerged tension leg platform for offshore wind turbines. Ocean Engineering, (2017) 129, 68-82.

[33] Bossanyi, E. A., Wind turbine control for load reduction. Wind Energy: An International Journal for Progress and Applications in Wind Power Conversion Technology, (2003) 6(3), 229-244.

[34] Jonkman, B.J., TurbSim User's Guide: Version 1.50. No. NREL/TP-500-46198. National Renewable Energy Lab. (NREL), Golden, CO (United States), 2009.

[35] Goupee, A.J., Kimball, R.W., Dagher, H.J., Experimental observations of active blade pitch and generator control influence on floating wind turbine response. Renew. Energy, (2017) 104, 9–19.

[36] Carlos Eduardo S. Souza, Erin E. Bachynski, Changes in surge and pitch decay periods of floating wind turbines for varying wind speed, Ocean Engineering, (2019) 180, 223-237.